Am J Transl Res 2023;15(1):125-137
www.ajtr.org /ISSN:1943-8141/AJTR0144993

Original Article

KCTD10 functions as a tumor suppressor in hepatocellular carcinoma by triggering the Notch signaling pathway

Tao Ma[1,3*], Daoyuan Wang[1,2*], Jiajun Wu[1,2*], Yihui Xiao[1,2], Anfang Fan[1,2], Xiaocheng Cao[1,2], Jianguo Cao[1,2], Kaiqun Ren[1,2]

[1]The Key Laboratory of Model Animals and Stem Cell Biology in Hunan Province, Medical College, Hunan Normal University, Changsha 410013, Hunan, China; [2]Key Laboratory of Study and Discover of Small Targeted Molecules of Hunan Province, Changsha 410013, Hunan, China; [3]Hunan Aerospace Hospital, No. 139 Fenglin Third Road, Yuelu District, Changsha 410205, Hunan, China. [*]Equal contributors.

Received June 27, 2022; Accepted December 1, 2022; Epub January 15, 2023; Published January 30, 2023

Abstract: Objective: Our previous study found KCTD10 negatively regulates Notch signaling, but whether KCTD10 regulates human hepatocellular carcinoma (HCC) carcinogenicity was uncertain. Methods: We used lentivirus infection to regulate KCTD10 expression in HCC cell lines, then monitored tumor sphere formation rate, cell migration, *in vitro* and *in vivo* tumorigenicity, cancer stem cell (CSC) biomarkers and Notch signaling variation. Results: Down-regulation of KCTD10 in HCC cell lines (Hep3B and MHCC97H) enhanced the expression of CSC marker genes, promoted self-renewal and tumorigenic ability, and increased the $CD133^+$ cell population. Further molecular studies showed that the transmembrane/intracellular region (NTM) of Notch1 decreased when KCTD10 was knocked down in HCC cell lines, and that the balance between P53 and Notch activity was regulated. Conclusions: The results demonstrated that KCTD10 can act as a tumor suppressor in HCC cells through Notch signaling.

Keywords: KCTD10, hepatocellular carcinoma, Notch, Numb/P53 balance, tumor suppressor

Introduction

Hepatocellular carcinoma (HCC) is the fifth most common human tumor and has the highest mortality rate, with a five-year survival rate of 25%-39% and a recurrence rate of 80% [1-3]. There is a theory that HCC maintenance, therapeutic resistance, and tumor recurrence are highly correlated with HCC stem cells (HCSCs) or stem-like cells (HSLCs) [4, 5]. HCSCs or HSLCs are cell populations that express stem cell markers and are more malignant and have a higher capability for self-renewal compared to parental cell lines [6, 7]. Chemoresistance leads to HCSCs surviving after conventional treatments and ultimately being responsible for relapse [8]. As a result, HCSCs are crucial for liver cancer therapy and have become a therapeutic target of primary interest for drug discovery [9]. Therefore, the identification of key genes or molecular events underlying the progression of HCSC or HSLC is needed.

Previous reports have shown that KCTD10 is essential for mammalian development [10-13]. Further functional studies showed that KCTD10 interacts with proliferating cell nuclear antigen (PCNA) and plays an important role in DNA synthesis [12]. Its down-regulation impairs the proliferation of A549 lung cancer cells [11]. In gastrointestinal stromal tumors, inhibition of KCTD10 expression increased the tumor cell proliferation and invasion, suggesting that KCTD10 acts as a tumor suppressor [14]. Since KCTD10 can regulate the Notch signaling pathway [13, 15], we investigated whether knocking down KCTD10 in HCC cell lines could modulate the self-renewal ability of HSLCs and the tumorigenicity of HCC, as well as the Notch signaling pathway and the balance between Numb and P53 in these cancer cells.

Materials and methods

Reagents and antibodies

Dulbecco's modified Eagle's medium (DMEM), DMEM/F12 medium, trypsin-EDTA and penicillin/streptomycin were purchased from HyClone (Logan, Utah, USA). Fetal bovine serum (FBS) was purchased from Biowest (Cat. No. S1820-500). Anti-β-actin monoclonal antibody was obtained from Sigma-Aldrich (No. A5441-.2ML, St. Louis, MO, USA). Polyclonal anti-ABCG2 (Cat. No. AP1490b), anti-Nanog (Cat. No. 1486c), anti-BMI1 (Cat. No. AP8756a) and anti-ALDH1A1 (Cat. No. AP1465d) antibodies were obtained from WuXi AppTec. CD133/2-PE (Cat. No. 130-112-157) was purchased from MiltenyiBiotec Technology & Trading (Shanghai, China) Co., Ltd. The rabbit Notch1 antibody (Cat. No. D6F11) and Notch receptor interaction antibody sampler kit (Cat. No. #8658) were purchased from Cell Signaling Technology, Inc. Anti-P53 antibody was purchased from Cell Signaling Technology, Inc (Cat. No. #2425).

Cell culture and lentivirus infection

HCC cell lines MHCC97H and Hep3B were obtained from Shanghai Fu Cheung Biological Technology Co., Ltd. (Shanghai, China), and cell lines LX2, HepG2, and Huh7 were obtained from Bogu Biotechnology (Shanghai, China). Cells were cultured in DMEM containing high glucose and 10% FBS at 37°C in a humidified incubator with 5% CO_2. KCTD10 interference short hairpin RNA (shRNA) sequence (CCAGCAAUUCUGACGACAATTUUGUCGUCAGAAUUGCUGGTA) was used to generate KCTD10 knockdown HCC cells. Negative control sequence (TTCTCCGAACGTGTCACGT) and KCTD10 cDNA were synthesized to construct ADV1 (U6/CMV-GFP)-KCTD10-shRNA, ADV1 (U6/CMV-GFP)-Lenti-NC, and ADV1 (U6/CMV-GFP)-KCTD10 lentiviruses produced by Suzhou Ji Kai Gene Technology Co., Ltd. (Suzhou, China). MHCC97H and Hep3B cells were infected with lentiviruses expressing KCTD10 shRNA, or a negative control sequence, or KCTD10 cDNA in the presence of 5 μg/ml polybrene. Twenty-four hours after infection, the cell supernatant was replaced with normal culture media.

Western blotting

Cells were washed with PBS and mixed with appropriate RIPA buffer (Solebo, Cat. No. R0020), supplemented with 1% PMSF (Biyun Sky, Cat. No. P1005). After incubation on ice for 30 min, cell lysates were centrifuged at 12000 × g for 5 min at 4°C to obtain whole cell extracts. A BCA assay kit (Vazyme, Cat. No. E112-01) was used to determine protein concentration. Proteins were resolved by 10% SDS-polyacrylamide gel electrophoresis and transferred to a polyvinylidene difluoride membrane (PVDF, Millipore, Billerica, MA, USA). The membrane was incubated overnight at 4°C with the primary antibody, washed six times with TBST, and incubated for one hour with goat anti-mouse IgG antibody or goat anti-rabbit IgG antibody coupled to horseradish peroxidase-coupled. The band signal was detected using an enhanced ECL chemiluminescence detection kit (Vazyme, Cat. No. E411-05).

Extraction of RNA and quantitative real-time PCR

Total RNA from HCC cell lines was extracted with TRIzol reagent (Invitrogen, Carlsbad, CA), and reverse transcription was performed with a cDNA first-strand synthesis kit (Roche Diagnostics, IN) according to the manufacturer's instructions. Real-time PCR analysis was performed using SYBR Green Supermix (Bio-Rad) and a C1000 Thermal Cycler (Bio-Rad). All data were normalized to the *36b4* gene. Primers were designed as follows: *Kctd10* forward 5'-CGTACCAAAGTGCTTCCCAC-3'; *Kctd-10* reverse 5'-CTATACCACCATGCAGACGC-3'; *Nanog* forward 5'-CCAGCTGTGTGTACTCAATAGTAG-3'; *Nanog* reverse 5'-ATTGTCATTCTTCGGCCAGTTG-3'; *Bmi1* forward 5'-GTTTCCTCACATTTCCAGTACTATG-3'; *Bmi1* reverse 5'-TTCCTTAACAGTCTCAGGTATCAAC-3'; *Cd133* forward 5'-ACCCAACATCATCCCTGTTCTTG-3'; *Cd133* reverse 5'-GCTGGTCAGACTGCTGCTAAG-3'; *Otc4* forward 5'-GTGGTCCGAGTGTGGTTCTGT-3'; *Otc4* reverse 5'-GCATAGTCGCTGCTTGATCG-3'; *36b4* forward 5'-AGATGCAGCAGATCCGCAT-3'; *36b4* reverse 5'-GTTCTTGCCCATCAGCACC-3'.

Sphere formation assay

HCC cells were plated in ultra-low attachment 6-well plates (5×10^3, 1×10^4 and 2×10^4 cells per well) for regular sphere formation in stem cell medium (SC-M) containing DMEM/F12 (Gibco, Invitrogen) plus 20 ng/mL EGF (PeproTech, NJ, USA), 10 ng/mL bFGF (PeproTech, NJ, USA), 1 × B27 (Invitrogen, CA, USA) and 0.4 μg/mL insulin (PeproTech). The number

of spheres was counted after one week under a microscope (IX71, Olympus, Japan).

Colony formation assay

Colony formation assay was performed to monitor the ability of HCC cells to form colonies. The single-cell suspension was seeded into a 6-well plate with DMEM plus 10% FBS at a density of 5 × 10^3 cells/per well. Cells were incubated at 37°C in a CO_2 incubator for two weeks, and colonies were stained with Giemsa and observed under a microscope (SZX16, Olympus, Japan). Each sample was analysed in triplicate, and this experiment was repeated three times.

Cell viability assay

Cell viability was determined using the Cell Counting Kit-8 (CCK-8) assay. Cells were seeded in 96-well plates at a density of 2 × 10^3 per well. After 24 hrs, 48 hrs, and 72 hrs of culture, 10 μL CCK-8 reagent was added to each well. After an additional 2 hrs of culture, cell supernatant was detected at 450 nm by the Synergy Multifunctional enzyme labeling instrument (Biotek Synergy 2, USA).

Wound-healing migration assays

Hep3B and MHCC97H cells were cultured in 24-well plates until reaching 90% confluence. A 100-μl pipette tip was used to generate wounds. After wound generation, cells were washed twice and changed to medium containing 2% serum. Three wound areas in each well were marked on the bottom of the plates and imaged at 0 and 24 hrs after wound formation with an inverted microscope (Olympus IX71, Japan).

In vivo tumorigenicity assay

Four-week-old BALB/c-nu mice weighing 12-14 g were purchased from Nanjing University Institute of Biopharmaceuticals (SCX (Su) 2018-0008). Then, the mice were housed on a normal 12 hr/12 hr light/dark cycle with ad libitum access to regular mouse chow and water in a specific pathogen-free facility (SYXK (Xiang) 2019-0008). Animal welfare and experimental procedures were carried out strictly in accordance with the Guide for the Care and Use of Laboratory Animals (National Research Council, 1996). All animals were carefully monitored, and animal ethics board approved of the research. All experiments on mice were based on protocol standards approved by the Ethics Committee of Hunan Normal University and the Board of Laboratory Animal Feeding and Use Management Committee (approval No. 2015-146). Animals were randomly divided into 2 groups. For group 1 (n = 3), 1 × 10^7 MHCC97H cells infected with either lentivirus with empty vector (Lenti-NC) or lentivirus with GFP-fused KCTD10 silencing RNA sequence (Lenti-KCTD10 Si) were taken separately and mixed with an equal part of Matrigel (Corning, Germany) and then injected subcutaneously near the left or right forelimb separately. For group 2 (n = 7), mice were inoculated with 1 × 10^7 cells that infected with lentivirus containing Lenti-KCTD10 Si near the left forelimb, and cells infected with lentivirus, containing Lenti-KCTD10 Si followed by lentivirus containing GFP-fused KCTD10 cDNA and overexpressing KCTD10 (Lenti-KCTD10 Si-OE) were inoculated near the right forelimb. Tumor volume was monitored twice weekly after inoculation according to the formula V (xenograft volume, mm^3) = π (6 × L × W × H), where L, W, and H represent the tumor length, width, and height, respectively. At the end of the experiment, the xenograft-bearing BALB/c-nu mice were sacrificed by CO_2 asphyxiation, and the tumor samples were collected and fixed in 10% neutral formalin.

Flow cytometry

MHCC97H cells were analyzed by flow cytometry with anti-CD133 antibody. Cells were suspended in PBS at a density of 1 × 10^6 cells/ml. After centrifugation, the supernatant was discarded, and the cells were resuspended in PBS supplemented with 5% BSA and then incubated for 10 minutes at 4°C with CD133/2-PE antibody (Metropolitan. Cat. No. 130-112-157). The percentage of $CD133^+$ cells was counted by BD FACS Calibur, and the data were analyzed by BD FACS Diva 8.0.1 (BD CantoII, USA).

Statistical analysis

Statistical analyses were performed using SPSS 20.0 software (IBM, Armonk, NY, USA) and SigmaPlot 12.5 (Systat Software Inc., San Jose, CA, USA). Data are represented as mean ± standard error of the mean (SEM). To test for

differences between groups, we used an unpaired two-tailed Student's t test to compare the different groups with controls. For the pairwise comparison among groups, we used the one-way test ANOVA followed by post-hoc Tukey's test. $P<0.05$ was considered significant.

Results

Knockdown of KCTD10 promotes self-renewal of HCC cells

To determine the significance of KCTD10 expression in HCC, we determined mRNA levels by quantitative PCR (**Figure 1A**) and protein levels by western blotting (**Figure 1B**) in HCC cell lines HepG2, Hep3B, Huh7, and MHCC97H. We found that KCTD10 was highly expressed in Hep3B, Huh7, and MHCC97H cells, so we decreased the levels of KCTD10 in Hep3B and MHCC97H cells to explore its biological function. After validating the silencing efficacy of KCTD10 shRNA on both the mRNA and protein levels of KCTD10 (**Figure 1C-F**), we first determined whether KCTD10 affects the characteristics of HCSCs. A typical feature of HCSCs is their ability to form three-dimensional structures or spheres in conditioned media, which is also referred to as self-renewal ability. To analyze the effects of KCTD10 on the self-renewal ability of HSLC, Hep3B, and MHCC97H cells transfected with either Lenti-KCTD10 Si or Lenti-NC were cultured in 6-well ultra-low attachment plates containing CSC-CM. The number of spheres in each group of cells was counted after one week. We found that the number of tumor spheres in the first-, second-, and third-generation Lenti-KCTD10 Si cell populations was approximately twice that in the Lenti-NC group in both Hep3B (**Figure 1G**, **1H**) and MHCC97H cells (**Figure 1G**, **1I**). These results suggest that inhibition of KCTD10 increases the self-renewal ability of HCC cells *in vitro*. These results demonstrate that KCTD10 inhibits the properties of HCC stem cells (HCSCs) or stem-like cells (HSLCs).

Knockdown of KCTD10 promotes in vitro tumorigenic potential of HCC cells

Tumorigenic potential is one of the characteristics of HCSCs. We next examined the effects of KCTD10 inhibition on the tumorigenic potential of Hep3B and MHCC97H cells (untreated) and lentivirus-infected cells using a colony formation assay on plates. There wano significant difference in colony formation rate between untreated cells and cells infected with Lenti-NC. The number of colonies in Lenti-KCTD10 Si cells increased 4-fold compared to Lenti-NC and untreated Hep3B cells (**Figure 2A**, **2B**), and the increase was 2-fold in MHCC97H cells (**Figure 2A-C**), suggesting that KCTD10 inhibition may increase the tumorigenic potential of HCC cells *in vitro*. We also used a CCK-8 assay to test cell viability after KCTD10 knockdown in Hep3B cells. We found that the OD_{450} level was statistically higher in the Lenti-KCTD10 Si groups than in the uninfected cells (mock) or the Lenti-NC groups at 24 hrs, 48 hrs, and 72 hrs (**Figure 2D**). Our results indicate that inhibition of KCTD10 levels promotes the proliferation and tumorigenic potential of HCC cells *in vitro*.

Knockdown of KCTD10 promotes HCC cell migration of in vitro

We next examined the effect of KCTD10 on HCC cell migration by wound healing assay. As shown in **Figure 3**, knockdown of KCTD10 resulted in a migration distance twice that of mock or Lenti-NC Hep3B cells (**Figure 3A**, **3C**). In MHCC97H cells, the migration distance in Lenti-KCTD10 Si cells was three times that of Lenti-NC cells (**Figure 3B**, **3D**). Thus, the above data show that knocking down KCTD10 can significantly increase the motility of HCC cells.

Knockdown of KCTD10 promotes tumorigenicity of MHCC97H cells in vivo

1×10^7 MHCC97H cells infected with Lenti-KCTD10 Si or Lenti-NC were injected subcutaneously into nude mice, and the mice were observed for tumor formation and growth. **Figure 4** shows that all mice injected with MHCC97H cells infected with Lenti-NC (in the left dorsal regions) and Lenti-KCTD10 Si (in the right dorsal regions) were able to form xenograft tumors. However, tumor size and tumor weight increased 30% in the Lenti-KCTD10 Si group compared to the Lenti-NC group (**Figure 4A**, **4B**). The tumors were visible at day 18 post inoculation and were almost the same size, but at day 24 after inoculation, they were slightly larger in the MHCC97H cells infected with Lenti-KCTD10 Si. At day 30 after inoculation, the tumor volume of MHCC97H cells

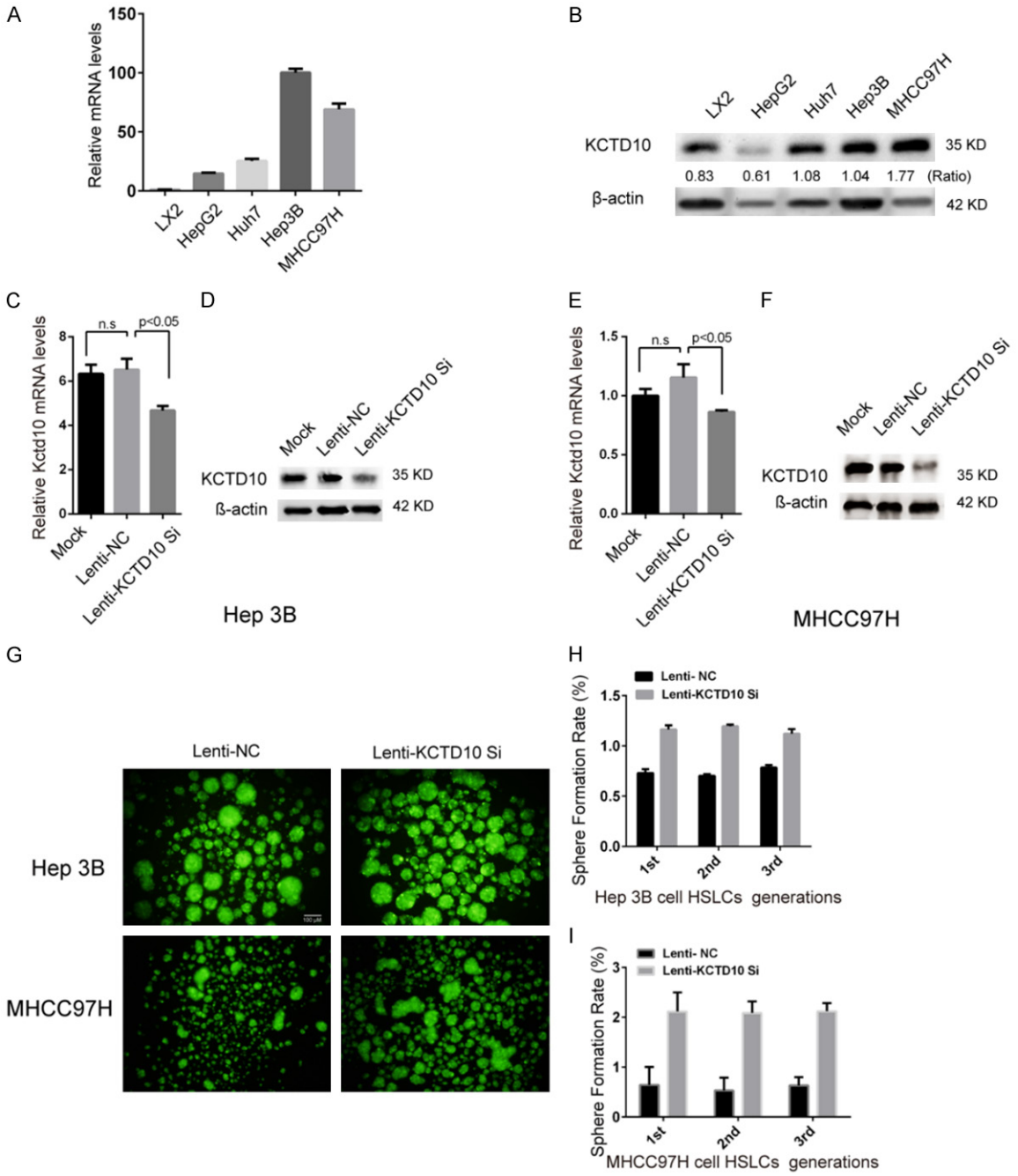

Figure 1. Inhibition of KCTD10 promotes self-renewal ability in HCC cells. (A) RT-PCR shows the relative mRNA levels of KCTD10 in hepatocellular cancer cell lines. (B) KCTD10 protein levels in different hepatocellular cancer cell lines were detected by western blotting. β-actin was used as an internal control. Quantitative PCR (C) and western blotting (D) were performed to examine KCTD10 mRNA and protein levels in Hep3B cells (Mock) or the cells infected with Lenti-KCTD10 Si or Lenti-NC; (E) Quantitative PCR was performed to check KCTD10 mRNA levels in cell populations of Mock, Lenti-NC, and Lenti-KCTD10 Si cell populations in MHCC97H cells; (F) In MHCC97H cells, KCTD10 protein levels in Mock, Lenti-NC and Lenti-KCTD10 Si cell populations were measured by western blotting, β-actin was used as an internal control; (G) Sphere formation assay for cells transfected with Lenti-NC or Lenti-KCTD10 Si in Hep3B and MHCC97H cells. Scale bars, 100 μm; (H) Statistics of the number of the first-, second- and third-generation spheres formed in Hep3B cells; (I) Number statistics of the first-, second- and third-generation spheres formed in MHCC97H cells. (A, C, E) Relative mRNA values represented as mean ± SEM of three independent experiments performed in triplicate. (H, I) Relative sphere formation rates, shown as mean ± SEM of three independent experiments performed in triplicate. Statistical test used: unpaired two-tailed Student's t-test. *, $P<0.05$.

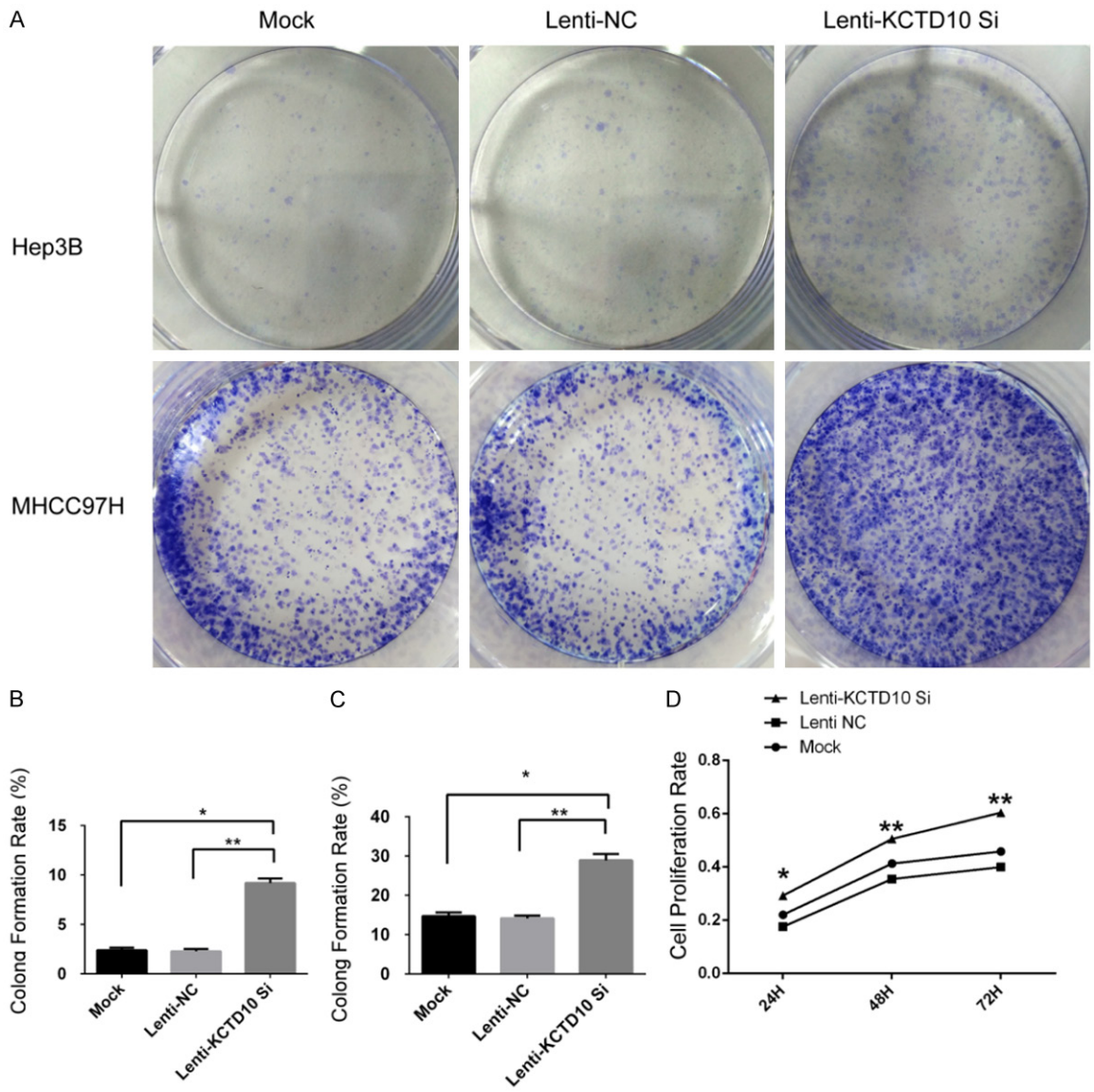

Figure 2. Knockdown of KCTD10 increases the colony formation rate in HCC cells. A. Colony formation assay in untreated cells (Mock) or in cells infected with Lenti-NC or Lenti-KCTD10-Si in both Hep3B cells and MHCC97H cells. B. Number of colonies formed in Hep3B cells upon inhibition of KCTD10 expression. C. Number of colonies formed in MHCC97H cells under inhibition of KCTD10 expression. B, C. Relative colony formation rates represented as mean ± SEM of three independent experiments performed in triplicate. Statistical tests used: unpaired two-tailed Student's t-test. *, *P*<0.05, **, *P*<0.01. D. Cell proliferation rate in Hep3B cells and KCTD10 knockdown cells (n = 5). Data are shown as mean ± SEM. Statistical test: unpaired two-tailed Student's t-test. *P<0.05, **, *P*<0.01 compared to Mock at each time point.

infected with Lenti-KCTD10 Si increased by approximately 40% compared to the Lenti-NC group (**Figure 4C**). As a result, the mice in the Lenti-KCTD10 Si group had a higher tumor burden than the mice in the Lenti-NC group (**Figure 4D**). These results demonstrate that knocking down KCTD10 promotes the *in vivo* tumorigenicity of MHCC97H cells in nude mice.

Re-expression of KCTD10 abrogates the promoting effect of KCTD10 knockdown on in vivo tumorigenicity of MHCC97H cells

To further confirm the effects of KCTD10 on tumorigenesis in MHCC97H cells, we re-expressed KCTD10 in MHCC97H cells infected with Lenti-KCTD10 Si (Lenti-KCTD10 Si-OE),

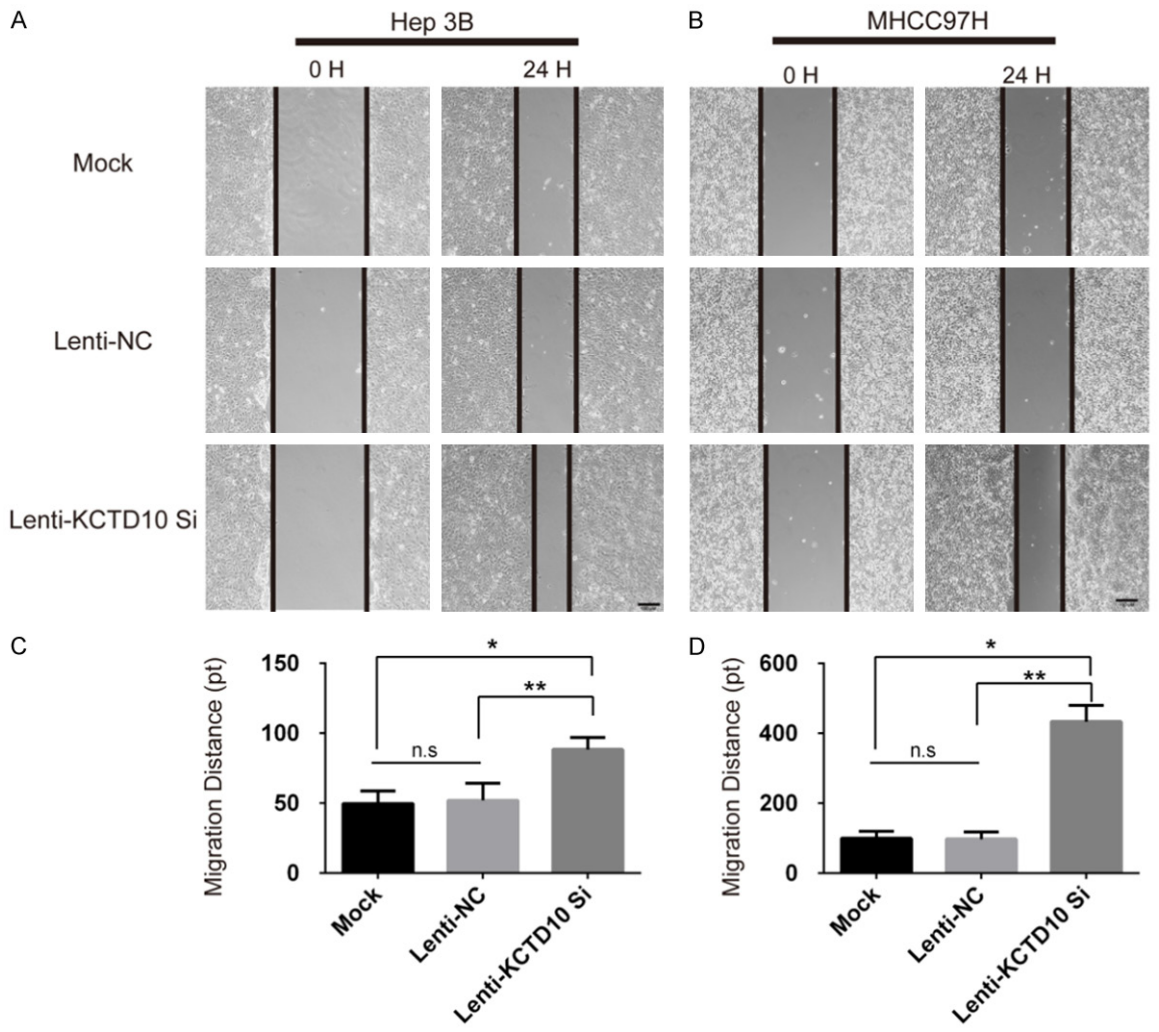

Figure 3. Knockdown of KCTD10 promotes cell migration in HCC cells. (A, B) Representative images of wound healing assays were acquired at the indicated time points after the onset of the scoring in lentivirus-infected and parental Hep3B cells (A) as well as in MHCC97H cells (B). Scale bars, 100 μm. (C, D) Relative migration distance represented as mean ± SEM of three independent experiments performed in triplicate of Hep3B cells (C) and MHCC97H cells (D). Statistical tests used: unpaired two-tailed Student's t-test. *, $P<0.05$, **, $P<0.01$.

injected these cells into nude mice, and monitored the mice for tumor formation and growth. The tumors in mice injected with Lenti-KCTD10 Si-OE cells were much smaller than those in mice injected with Lenti-KCTD10 Si cells (**Figure 5A**, **5B**). The tumor volume (**Figure 5C**) ($P<0.05$) and weight (**Figure 5C**, **5D**) ($P<0.05$) were much smaller in the Lenti-KCTD10 Si-OE group than in the Lenti-KCTD10 Si group. We also measured the protein levels of KCTD10 in these two MHCC97H cell groups (Lenti-KCTD10 Si and Lenti-KCTD10 Si-OE) by WB analysis, and the results showed that the protein levels in the Lenti-KCTD10 Si-OE groups were similar to those in the negative control groups (Lenti-KCTD10 NC) after the rescue experiment by re-expression (**Figure 5E**). Our results clearly demonstrate that KCTD10 can effectively inhibit the *in vivo* tumorigenicity of HCC cells in a nude mouse model.

Knockdown of KCTD10 increases the expression of HCSC biomarkers

Given the above results that inhibition of KCTD10 increases the tumorigenic potential of HCC cells *in vitro* and *in vivo*, we asked whether KCTD10 regulates HCSC cells. As shown in **Figure 6A**, of the four CSC marker genes tested, *Cd133* mRNA levels were three folds higher in cell populations knocking down KCTD10 (Lenti-KCTD10 Si) than those of

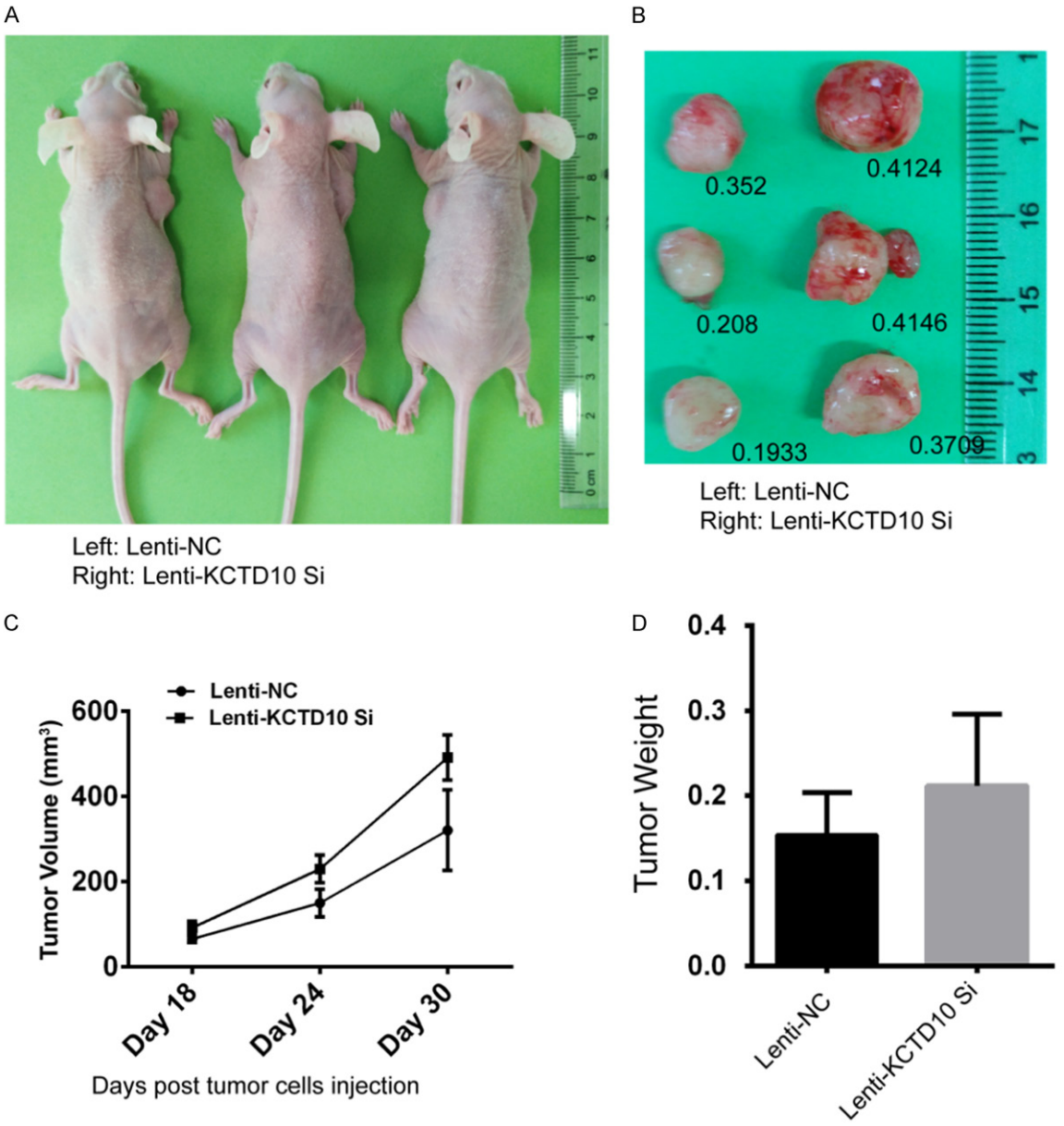

Figure 4. Knockdown of KCTD10 promotes tumorigenicity of MHCC97H cells *in vivo* in nude mouse model. A. MHCC97 cells infected with lentivirus containing empty vector (Lenti-NC), or GFP fused KCTD10 silent RNA sequence fused with GFP (Lenti-KCTD10 Si) were injected into the left or right forelimb of nude mice separately. Mice were photographed 31 days after inoculation; B. Tumor weights were measured 31 days after tumor cells injection. Left: Lenti-KCTD10 NC-MHCC97H cells. Right: Lenti-KCTD10 Si MHCC97H cells; C. Tumor volumes were measured at day 18, 24, 30 post tumor cells injection. D. Tumor weights were calculated at 31 days after tumor cells injection. Results are presented as mean ± SD, n = 3. Scale bars, upper panel = 3.5 cm, lower panel = 2.5 cm. *P<0.05, **P<0.01, unpaired t test.

mock or Lenti-NC-infected cells, as were *Oct4, Bmi1,* and *Nanog*. Western blotting analysis showed that protein levels of ALDH1 and Nanog were higher in Lenti-KCTD10 Si cells than in mock and Lenti-NC-infected cells (**Figure 6B**). Notably, the percentage of $CD133^+$ cells increased from 87% to 94.3% (**Figure 6C**). These results demonstrate that inhibition of KCTD10 may alter the HCSC population of HCC cells.

Notch signaling pathway may be involved in modulation of HCC tumorigenicity by KCTD10

Our team and *Ye et al*. found that KCTD10 functions as a regulator of Notch signaling [13, 15].

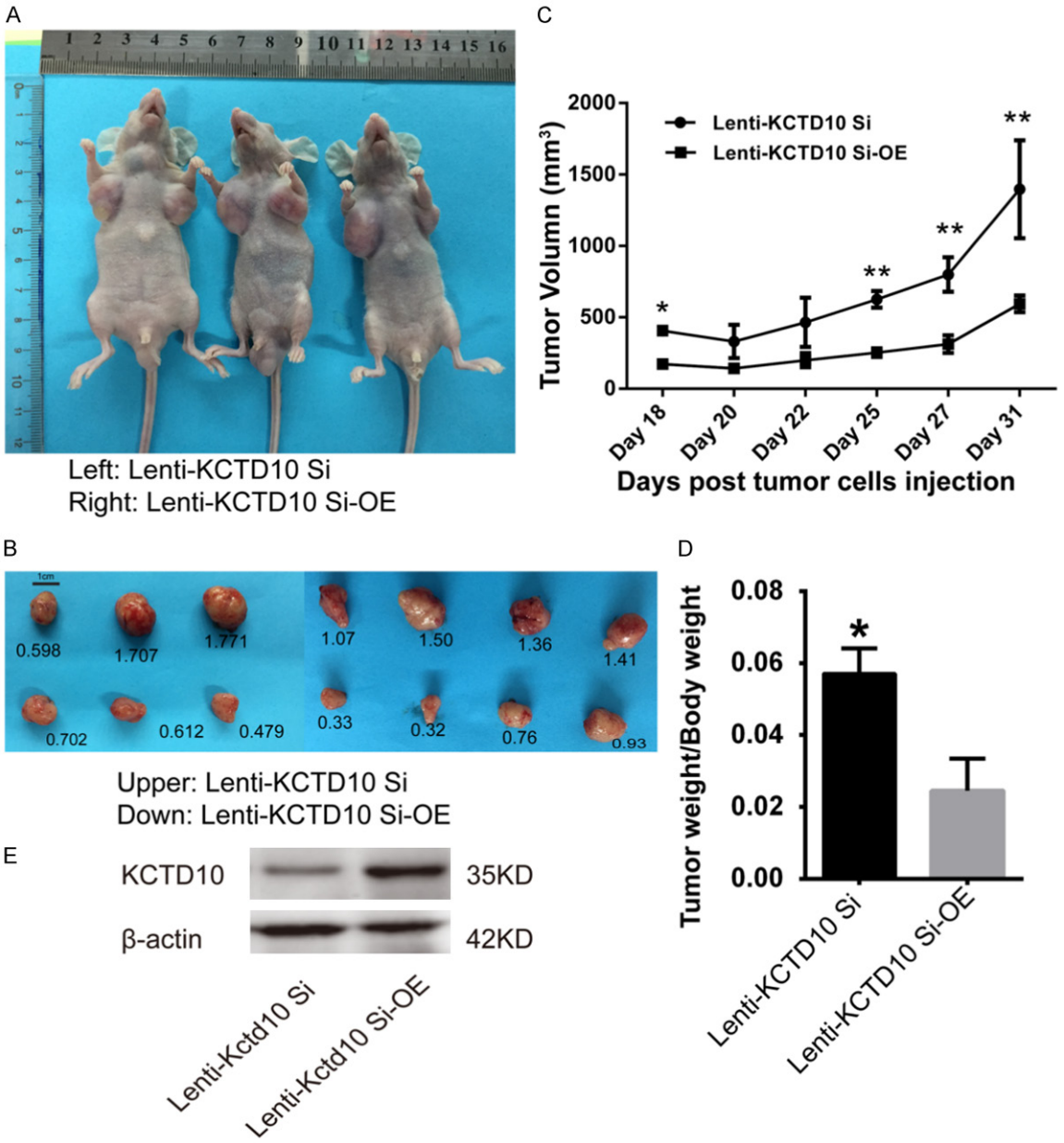

Figure 5. Re-expression of KCTD10 suppresses tumor growth in nude mice. A. Mice infected with Lenti-KCTD10 Si-MHCC97H cells and Lenti-KCTD10 Si-OE-MHCC97H cells (5.0×10^7) were photographed at day 31 after inoculation. B. Mice were euthanized and tumor weights were measured. Upper: tumor tissues inoculated with Lenti-KCTD10 Si-MHCC97H cells. Lower: tumor tissues inoculated with Lenti-KCTD10 Si-OE-MHCC97H cells; C. Tumor size was measured at an interval of two weeks after inoculation; D. Tumor weights/body weights were calculated when mice were euthanized on day 31 post-injection. Results are presented as mean ± SEM, n = 7. Scale bars, upper panel = 3.5 cm, lower panel = 2.5 cm. *P<0.05, **P<0.01, unpaired t test. E. Protein levels of KCTD10 in groups of cells infected as a negative control (Lenti-NC), Lenti-KCTD10 Si, and Lenti-KCTD10 Si-OE were detected by western blot.

Notch signaling may promote oncogenesis by activating liver progenitor cells [16]. Therefore, we investigated whether Notch signaling is affected by knocking down of KCTD10 in HCC cells. When KCTD10 was silenced in Hep3B cells, protein levels of Notch ligands Jagged1 and Jagged2 were up-regulated. However, RBPSUH (Recombining Binding Protein, Suppressor of Hairless, also referred to as RBP-J or CSL), which functions as the DNA-binding component of the transcriptional complex regulated by canonical Notch signaling, was slightly down-regulated when KCTD10 was partially silenced (**Figure 7A**). In MHCC97H cells, protein

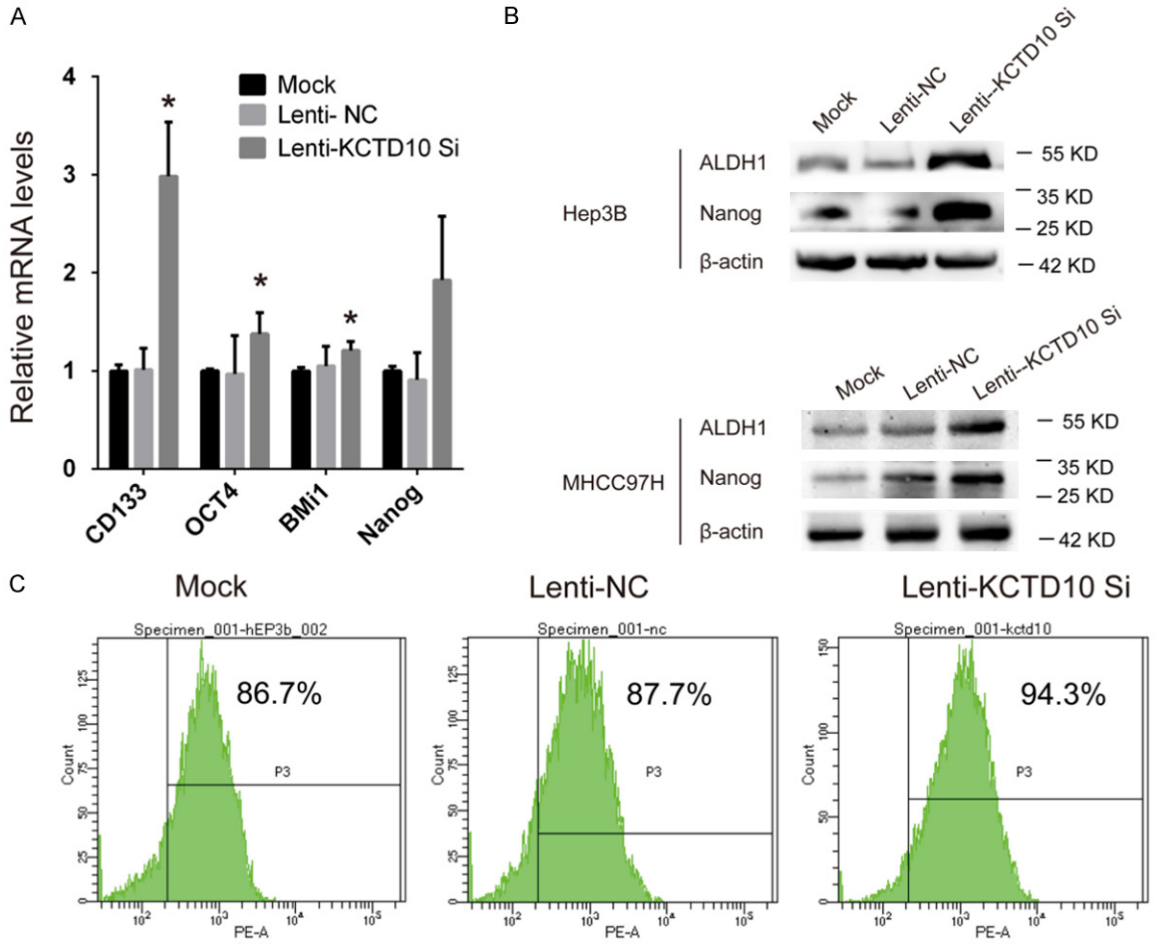

Figure 6. Knockdown of KCTD10 increases the expression of HCSC markers. A. mRNA levels of *Cd133*, *Oct4*, *Bmi1*, and Nanog in Mock, Lenti-NC, and Lenti-KCTD10 Si cells by qPCR. Relative mRNA levels are shown as mean ± SEM of three independent experiments performed in triplicate. Statistical tests used: unpaired two-tailed Student's t-test. *, $P<0.05$. B. Western blot results show protein levels of ALDH1 and Nanog in Mock, Lenti-NC, and Lenti-KCTD10 Si cells separately. C. Flow cytometry analysis of the percentage of $CD133^+$ cell population in Mock, Lenti-NC, and Lenti-KCTD10 Si cells separately.

levels of the Notch ligand Jagged2 were not affected, but Jagged1, DLL1, DLL3, DLL4, and RBPSUH were significantly decreased when KCTD10 was knocked down (**Figure 7B**). In addition, we found that inhibition of KCTD10 could increase HES1 protein levels in both Hep3B and MHCC97H cells (**Figure 7C**). We then examined the differences between the molecular mechanisms of Hep3B and MHCC97H cells. In a previous publication, Notch signaling was shown to promote cholangiocarcinoma progression and was enhanced by P53 inactivation [17, 18]. We determined the expression status of P53 in various hepatocellular cell lines and found that P53 was highly expressed in MHCC97H cells but not in Hep3B cells (**Figure 7D**). Numb plays an important role in the activation of P53 [19]. In our experiment, P53-positive HCC cell lines exhibited increased Numb protein levels (**Figure 7D**). Taken together, our results showed that KCTD10 silencing increased Nanog and HES1 protein levels in both high-level P53-expressing and absent hepatocellular cell lines, but it decreased P53 protein levels, as well as increased Numb expression in high P53-expressing HCC cell lines, suggesting that KCTD10 may play an important role in maintaining the balance between P53 and Notch activity and has important implications for HCSC homeostasis and tumorigenesis.

Discussion

The present study provides evidence that carcinogenicity and stem cell formation in HCC cells

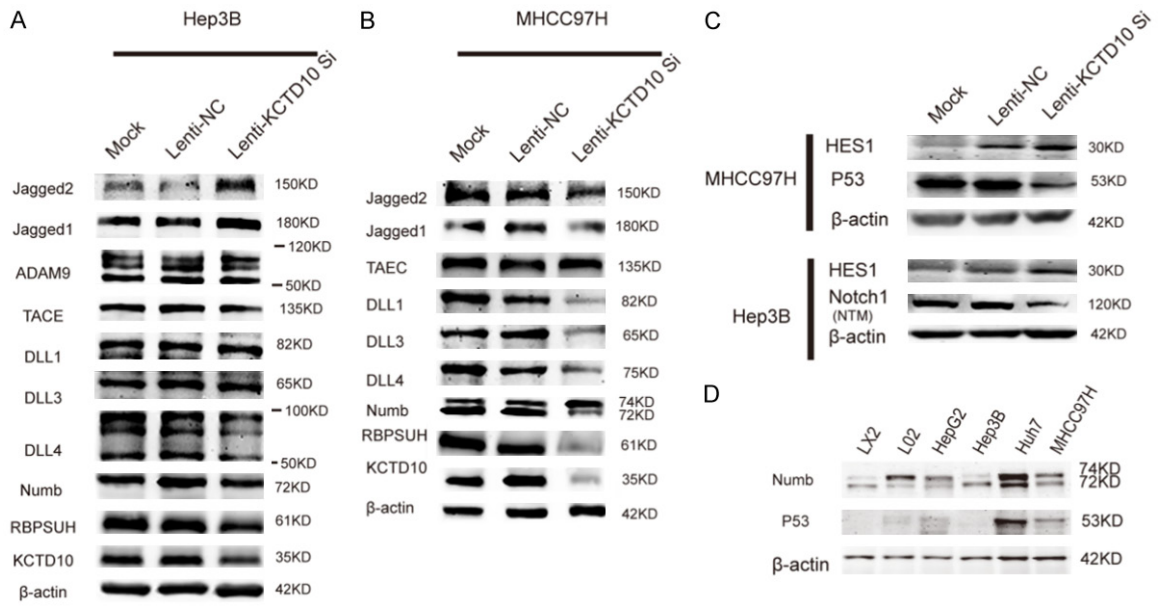

Figure 7. Inhibition of KCTD10 affects Notch signaling. A, B. Hep3B and MHCC97H cell lysates (100 μg) from Mock, Lenti-NC, or Lenti-KCTD10 Si cells were immunoblotted with Notch signaling antibodies. C. Lysates of Hep3B and MHCC97H cells (100 μg) from Mock, Lenti-NC, or Lenti-KCTD10 Si were immunoblotted with anti-HES1 and anti-P53 antibodies. D. Multiple lysates from hepatocellular cell lines (100 μg) were immunodetected by western blot with anti-P53 and anti-Numb antibodies separately. β-actin was used as a loading control.

can be inhibited by KCTD10. Knockdown of KCTD10 in HCC cell lines increased mRNA and protein levels of stem cell markers, promoted self-renewal and tumorigenic ability, and increased $CD133^+$ cell populations. As for the molecular mechanism, knocking down KCTD10 decreased the transmembrane/intracellular region (NTM) of Notch1 and the balance between P53 and Notch activity in HCC cell lines. These results suggest that KCTD10 may act as a tumor suppressor in HCC cells and regulate the balance between P53 and Notch activity.

KCTD10 belongs to the polymerase delta-interacting protein 1 (PDIP1) family, which interacts with proliferating cell nuclear antigen (PCNA) and DNA polymerase δ and plays a role in cell proliferation, including DNA synthesis, DNA repair, DNA methylation and cell division [12, 20]. Wang *et al*. showed that silencing KCTD-10 expression can inhibit cell proliferation in A549 lung adenocarcinoma cells [11]. Kubota *et al.* showed that silencing of KCTD10 promoted cell proliferation and invasion, suggesting that KCTD10 protein plays an inhibitory role in gastrointestinal tumor cells [14]. In this study, we inhibited the level of KCTD10 in HCC cells and found that this modulation increased the cells' self-renewal ability and tumorigenicity *in vitro* and *in vivo*. Consistent with the findings of Kubota *et al*., our results suggest that KCTD10 may be a tumor suppressor, and that inhibition of KCTD10 expression may increase stem-like properties and tumorigenicity [14].

Notch signaling is multifaceted and highly context-dependent in cancer development; it may have opposite functions at different time points even within the same tissue [21, 22]. In liver cancer, Notch has been shown to act as a tumor suppressor by inhibiting the development of HCC [23]. However, two other research groups have suggested Notch to have increased activity in the progression of HCC [24, 25]. In our studies, inhibition of KCTD10 promoted HCC development accompanied by a decrease in protein levels of the Notch ligands Jagged1, DLL1, DLL3, and DLL4, suggesting that KCTD10 and the Notch ligands act as tumor suppressors in HCC. We tested two HCC cell lines based on the expression status of P53. MHCC97H cells, which have high P53 protein levels, showed decreased protein levels of Notch ligands after partial knockdown of

KCTD10. In addition, Hep3B cells lacking P53 showed increased Notch ligands Jagged1 and Jagged 2 when KCTD10 was knocked down, but no effect on other ligands.

Previous studies have shown that human Numb forms a complex with the tumor protein P53 and prevents its ubiquitination and degradation [19, 26, 27]. Importantly, higher Nanog expression leads to increased Numb phosphorylation and decreased P53 protein levels [28-30]. In our study, silencing of KCTD10 resulted in higher Nanog protein and mRNA levels and lower P53 protein levels, suggesting that KCTD10 modulates this molecular balance.

Currently, there are few studies on the function of KCTD10 in tumor cells, and the role of KCTD10 mechanisms in tumor cells is poorly understood. We found that the status of KCTD10 affects stem cell-like properties and tumorigenicity and modulates the balance between Numb and P53 and the Notch signaling pathway in HCC cells. Our findings provide a theoretical basis for future HCC therapy.

Acknowledgements

We acknowledge the support from the Key Laboratory of Model Animals and Stem Cell Biology in Hunan Province (2019TP1035) and the Key grant of research and development in Hunan Province (2020DK2002). This work was supported by the project of the National Natural Science Fund (No. 3150913), the Natural Science Foundation of Hunan Province (No. 2015JJ6072, No. 2020JJ4441), and the Research Foundation of Education Bureau of Hunan Province, China (No. 20A304).

Disclosure of conflict of interest

None.

Address correspondence to: Kaiqun Ren and Jianguo Cao, The Key Laboratory of Model Animals and Stem Cell Biology in Hunan Province, Medical College, Hunan Normal University, Changsha 410013, Hunan, China. Tel: +86-731-88912434; Fax: +86-731-88912434; E-mail: kaiqunren@126.com (KQR); caojianguo2005@126.com (JGC)

References

[1] Sia D, Villanueva A, Friedman SL and Llovet JM. Liver cancer cell of origin, molecular class, and effects on patient prognosis. Gastroenterology 2017; 152: 745-761.

[2] Yan X and Qiu Y. Impact of current staging systems on treatment strategy for HBV-related hepatocellular carcinoma. Cancer Lett 2016; 379: 220-224.

[3] Thomas MB and Zhu AX. Hepatocellular carcinoma: the need for progress. J Clin Oncol 2005; 23: 2892-2899.

[4] Ghouri YA, Mian I and Rowe JH. Review of hepatocellular carcinoma: epidemiology, etiology, and carcinogenesis. J Carcinog 2017; 16: 1.

[5] Xu XL, Xing BC, Han HB, Zhao W, Hu MH, Xu ZL, Li JY, Xie Y, Gu J, Wang Y and Zhang ZQ. The properties of tumor-initiating cells from a hepatocellular carcinoma patient's primary and recurrent tumor. Carcinogenesis 2010; 31: 167-174.

[6] Collins AT, Berry PA, Hyde C, Stower MJ and Maitland NJ. Prospective identification of tumorigenic prostate cancer stem cells. Cancer Res 2005; 65: 10946-10951.

[7] Suetsugu A, Nagaki M, Aoki H, Motohashi T, Kunisada T and Moriwaki H. Characterization of CD133+ hepatocellular carcinoma cells as cancer stem/progenitor cells. Biochem Biophys Res Commun 2006; 351: 820-824.

[8] Pattabiraman DR and Weinberg RA. Tackling the cancer stem cells-what challenges do they pose? Nat Rev Drug Discov 2014; 13: 497-512.

[9] Marcucci F, Rumio C and Lefoulon F. Anti-cancer stem-like cell compounds in clinical development-an overview and critical appraisal. Front Oncol 2016; 6: 115.

[10] Sun JK, Zhang B, Zhang J and Zhou JL. Preparation of mouse KCTD10 antibody and expression analysis of KCTD10 in neuroepithelium of neural tube and dorsal root ganglion. Sheng Wu Gong Cheng Xue Bao 2007; 23: 1011-1016.

[11] Wang Y, Zheng Y, Luo F, Fan X, Chen J, Zhang C and Hui R. KCTD10 interacts with proliferating cell nuclear antigen and its down-regulation could inhibit cell proliferation. J Cell Biochem 2009; 106: 409-413.

[12] Zhou J, Ren K, Liu X, Xiong X, Hu X and Zhang J. A novel PDIP1-related protein, KCTD10, that interacts with proliferating cell nuclear antigen and DNA polymerase delta. Biochim Biophys Acta 2005; 1729: 200-203.

[13] Ren K, Yuan J, Yang M, Gao X, Ding X, Zhou J, Hu X, Cao J, Deng X, Xiang S and Zhang J. KCTD10 is involved in the cardiovascular system and Notch signaling during early embryonic development. PLoS One 2014; 9: e112275.

[14] Kubota D, Yoshida A, Tsuda H, Suehara Y, Okubo T, Saito T, Orita H, Sato K, Taguchi T, Yao T, Kaneko K, Katai H, Kawai A and Kondo T. Gene

expression network analysis of ETV1 reveals KCTD10 as a novel prognostic biomarker in gastrointestinal stromal tumor. PLoS One 2013; 8: e73896.
[15] Ye MS, Luo L, Guo Q, Su T, Cheng P and Huang Y. KCTD10 regulates brown adipose tissue thermogenesis and metabolic function via Notch signaling. J Endocrinol 2022; 252: 155-166.
[16] Geisler F and Strazzabosco M. Emerging roles of Notch signaling in liver disease. Hepatology 2015; 61: 382-392.
[17] El Khatib M, Bozko P, Palagani V, Malek NP, Wilkens L and Plentz RR. Correction: activation of Notch signaling is required for cholangiocarcinoma progression and is enhanced by inactivation of p53 in vivo. PLoS One 2018; 13: e0206953.
[18] El Khatib M, Bozko P, Palagani V, Malek NP, Wilkens L and Plentz RR. Activation of Notch signaling is required for cholangiocarcinoma progression and is enhanced by inactivation of p53 in vivo. PLoS One 2013; 8: e77433.
[19] Colaluca IN, Tosoni D, Nuciforo P, Senic-Matuglia F, Galimberti V, Viale G, Pece S and Di Fiore PP. NUMB controls p53 tumour suppressor activity. Nature 2008; 451: 76-80.
[20] Maga G and Hubscher U. Proliferating cell nuclear antigen (PCNA): a dancer with many partners. J Cell Sci 2003; 116: 3051-3060.
[21] Wilson A and Radtke F. Multiple functions of Notch signaling in self-renewing organs and cancer. FEBS Lett 2006; 580: 2860-2868.
[22] Liu J, Sato C, Cerletti M and Wagers A. Notch signaling in the regulation of stem cell self-renewal and differentiation. Curr Top Dev Biol 2010; 92: 367-409.
[23] Viatour P, Ehmer U, Saddic LA, Dorrell C, Andersen JB, Lin C, Zmoos AF, Mazur PK, Schaffer BE, Ostermeier A, Vogel H, Sylvester KG, Thorgeirsson SS, Grompe M and Sage J. Notch signaling inhibits hepatocellular carcinoma following inactivation of the RB pathway. J Exp Med 2011; 208: 1963-1976.
[24] Kawaguchi K, Honda M, Yamashita T, Okada H, Shirasaki T, Nishikawa M, Nio K, Arai K, Sakai Y, Mizukoshi E and Kaneko S. Jagged1 DNA copy number variation is associated with poor outcome in liver cancer. Am J Pathol 2016; 186: 2055-2067.
[25] Ma L, Dong P, Liu L, Gao Q, Duan M, Zhang S, Chen S, Xue R and Wang X. Overexpression of protein O-fucosyltransferase 1 accelerates hepatocellular carcinoma progression via the Notch signaling pathway. Biochem Biophys Res Commun 2016; 473: 503-510.
[26] Nayak RC, Hegde S, Althoff MJ, Wellendorf AM, Mohmoud F, Perentesis J, Reina-Campos M, Reynaud D, Zheng Y, Diaz-Meco MT, Moscat J and Cancelas JA. The signaling axis atypical protein kinase C lambda/iota-Satb2 mediates leukemic transformation of B-cell progenitors. Nat Commun 2019; 10: 46.
[27] Wang X, Wang R, Bai S, Xiong S, Li Y, Liu M, Zhao Z, Wang Y, Zhao Y, Chen W, Billiar TR and Cheng B. Musashi2 contributes to the maintenance of CD44v6+ liver cancer stem cells via notch1 signaling pathway. J Exp Clin Cancer Res 2019; 38: 505.
[28] Siddique HR, Feldman DE, Chen CL, Punj V, Tokumitsu H and Machida K. NUMB phosphorylation destabilizes p53 and promotes self-renewal of tumor-initiating cells by a NANOG-dependent mechanism in liver cancer. Hepatology 2015; 62: 1466-1479.
[29] Webb LM, Oyesola OO, Früh SP, Kamynina E, Still KM, Patel RK, Peng SA, Cubitt RL, Grimson A, Grenier JK, Harris TH, Danko CG and Tait Wojno ED. The Notch signaling pathway promotes basophil responses during helminth-induced type 2 inflammation. J Exp Med 2019; 216: 1268-1279.
[30] Choi HY, Seok J, Kang GH, Lim KM and Cho SG. The role of NUMB/NUMB isoforms in cancer stem cells. BMB Rep 2021; 54: 335-343.